COMBINED LATTICE-BOLTZMANN AND MOLECULAR-DYNAMICS SIMULATION OF BIOPOLYMER TRANSLOCATION THROUGH AN ARTIFICIAL NANO-PORE

Suresh Alapati,[1] Sangmo Kang[2] and Yong Kweon Suh[*2]

나노 세공을 지나는 생체고분자 운동에 대한 격자-볼츠만과 분자동역학에 의한 수치해석

수레수알라파티,[1] 강상모,[2] 서용권[*2]

Translocation of biopolymers such as DNA and RNA through a nano-pore is an important process in biotechnology applications. The translocation process of a biopolymer through an artificial nano-pore in the presence of a fluid solvent is simulated. The polymer motion is simulated by Langevin molecular dynamics (MD) techniques while the solvent dynamics are taken into account by lattice-Boltzmann method (LBM). The hydrodynamic interactions are considered explicitly by coupling the polymer and solvent through the frictional and the random forces. From simulation results we found that the hydrodynamic interactions between polymer and solvent speed-up the translocation process. The translocation time τ_T scales with the chain length N as $\tau_T \propto N^{\alpha}$. The value of scaling exponents(α) obtained from our simulations are 1.29 ± 0.03 and 1.41 ± 0.03, with and without hydrodynamic interactions, respectively. Our simulation results are in good agreement with the experimentally observed value of α, which is equal to 1.27 ± 0.03, particularly when hydrodynamic interaction effects are taken into account.

Key Words : Langevin-dynamics, Lattice-Boltzmann method, Polymer translocation

1. INTRODUCTION

Soft condensed matter is described as the materials which are easily deformable by small amount of forces due to electrical or magnetic fields, or even thermal fluctuations. These substances include collides, polymers, gels, foams and number of biological materials. The length scales of this type of substances come in mesoscopic range (10-09m-10-06m), which is in between microscale(less than 10-10m) and macroscale (greater than 10-03m). Hydrodynamic interactions (interactions with solvent molecules) play an important role in simulation of the soft matter suspended in a fluid. There is a large difference in special and temporal scales between the soft matter and solvent molecules. The solvent particles moves very rapidly compared to polymers or colloids. For example, the diffusion time (relaxation time) of polymer is several orders of magnitude larger than the solvent time scale (10-12s). If we completely rely on molecular dynamics simulation, we have to consider so many solvent molecules even for small number of polymer particles and also the time scale of simulation is solvent time scale and most of the computational time is spent on details of the solvent which are of not our concern. To deal with this type of problems recently multiscale modeling techniques are developed which reduce the computational time up to two orders of magnitude. In these techniques the solvent is modeled on continuum basis and the

1 학생회원, 동아대학교 대학원 기계공학과
2 정회원, 동아대학교 기계공학과
* Corresponding author, E-mail: yksuh@donga.ac.kr

polymer is modeled by standard molecular dynamic techniques. The polymer and the solvent are coupled by a simple dissipative (hydrodynamic) force. There are so many mesoscopic methods are available for simulating solvent dynamics on continuum basis. Some of them are Brownian Dynamics (BD)[1], Dissipative Particle Dynamics (DPD)[2], Multiparticle Collision Dynamics (MPC)[3], and Lattice Boltzmann Equation (LBE)[4,5]. All these methods have their strengths and weaknesses. The advantage of LBE over other methods is that the computational cost of taking the hydrodynamic interaction effects scales only linearly with the length of the polymer.

Translocation of bio-polymer molecules through nanometer sized pores in a membrane is the most fundamental process in the fields of chemistry and biotechnology. This event often takes place in several biological processes such as DNA and RNA sequencing, proteins transporting trough a cell membrane, transfer of virus RNA to the host cells, Gene therapy, gel electrophoresis, delivery of drug molecules to their activation sites etc. Therefore understanding the translocation phenomenon might lead to develop new and improved techniques for biological applications. Many researchers paid considerable attention in this topic to know the underlying physics by theoretically, experimentally and numerically. However, still there is a scope for further research. Theoretical predictions of translocation dynamics are very difficult as there are so many factors affecting the entire process. The main factors that affecting the translocation process are: interactions between monomers in the polymer chain, hydrodynamic interactions, driving force (electrical or chemical potential difference), concentration gradient of the polymer, pore size and polymer size. The main object of this work is to know the effect hydrodynamic interactions on translocation process. The paper is organized as follows: The details of numerical method are given in section 2. The results obtained from the simulation of translocation process are presented in section 3. Finally, in section 4 the conclusions of the present study are drawn.

2. NUMERICAL METHOD

2.1 MODELING THE POLYMER

The polymer is represented by bead-spring model, consists of N monomer units (also referred as beads) which are connected by N-1 flexible springs. The force acting on each bead can be represented by using the generalized Langevin equations of motion for bead positions $\boldsymbol{r_i}$ and velocities $\boldsymbol{v_i}$ for $i = 1,...,N$,

$$\frac{d\boldsymbol{r_i}}{dt} = \boldsymbol{v_i} \tag{1a}$$

$$m_i \frac{d\boldsymbol{v_i}}{dt} = -\nabla_i \vartheta(\boldsymbol{r_i})_{total} + \boldsymbol{F_{drag,i}} + \boldsymbol{F_{ran,i}}. \tag{1b}$$

where $\vartheta(\boldsymbol{r_i})_{total}$ represents the total potential energy of the system consists of Lennard-Jones potential, Coulomb potential, bond potential, and external electric field potential etc. $\boldsymbol{F_{drag,i}}$ in Eq. (1b) represents the dissipative drag force due to the motion of the polymer in a continuum fluid, and is given by

$$\boldsymbol{F_{drag,i}} = -m_i\gamma(\boldsymbol{v_i} - \boldsymbol{u_i}) \tag{2}$$

where m_i is the mass of the bead, γ the friction coefficient and $\boldsymbol{u_i}$ the velocity of the fluid evaluated at the bead position. If there is no hydrodynamic interactions effect, we just set $\boldsymbol{u_i} = 0$. $\boldsymbol{F_{ran,i}}$ in Eq. (1b) is a random force due to the thermal fluctuations in the fluid environment, which is taken as Gaussian white noise term obeying the following properties:

$$\begin{aligned} &< \boldsymbol{F_{ran,i}} > = 0, \\ &< \boldsymbol{F_{ran,i}}\boldsymbol{F_{ran,j}} > = 2mk_BT\gamma\delta_{ij}\delta(t-t'). \end{aligned} \tag{3}$$

In Eq. (3) the coupling between the temperature k_BT and γ is a result of fluctuation dissipation theorem (FDT) to keep the polymer beads and solvent molecules at the same temperature.

The excluded volume effect between bead-bead, and between bead-wall are taken by standard 6-12 Lennard-Jones potential [6],

$$V_{LJ}(\boldsymbol{r}) = 4\epsilon\left[\left(\frac{\sigma}{\boldsymbol{r}}\right)^{12} - \left(\frac{\sigma}{\boldsymbol{r}}\right)^{6}\right] \tag{4}$$

truncated at a distance of $\boldsymbol{r} = 2^{1/6}\sigma$. Here $\boldsymbol{r}$ is the distance between two beads or distance between bead and wall molecules, σ the length scale, and ϵ the energy scale of the system, respectively. The effect of electrostatic interactions is not included in the simulations. The connectivity between adjacent beads i and j is given by harmonic bond stretching potential,

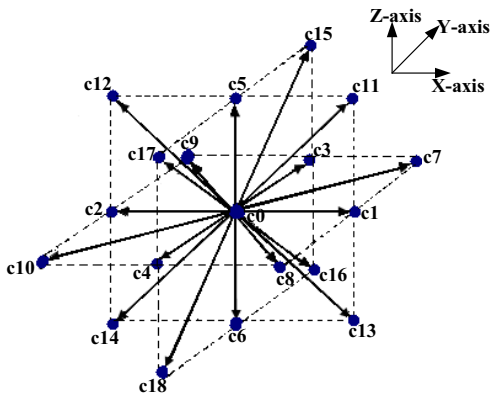

Fig. 1 D3Q19 (3D with 19 velocity vectors) lattice.

$$V_{bond}(\boldsymbol{r}) = \frac{1}{2} K_{bond}(\boldsymbol{r_{ij}} - \boldsymbol{r_{eq}})^2 \tag{5}$$

where K_{bond} is force constant and $\boldsymbol{r_{eq}}$ is the equilibrium distance between adjacent beads. The effect of bond angle potential is ignored as we assume the polymer of being flexible in nature.

2.2 Modeling the Solvent

The solvent is modeled by lattice Boltzmann method (LBM)[7]. In LBM, the hydrodynamic variables (density, velocity) are evaluated from the particle distribution functions, $f_i(\boldsymbol{r},t)$, by numerically solving the Boltzmann kinetic equation on a discrete lattice mesh. Here $f_i(\boldsymbol{r},t)$ represents the probability of finding a particle at lattice site $\boldsymbol{r}$ and at time t which is moving with discrete velocity $\boldsymbol{c_i}$. The particles move on a regular lattice defined by discrete velocity set $\boldsymbol{c_i}$(i=1,....,b), which is chosen such that after the time step $\triangle t$, the vector $\boldsymbol{c_i}\triangle t$ is leading to the ith neighbor on the grid. Here we worked with a cubic lattice consisting of 19 velocity vectors in 3-dimensions (D3Q19 lattice, see fig. 1). The evolution of f_i is governed by generalized lattice Boltzmann equation [8]:

$$f_i(\boldsymbol{r}+\boldsymbol{c_i}\triangle t, t+\triangle t) = f_i^*(\boldsymbol{r},t) = f_i(\boldsymbol{r},t) + \sum_{j=1}^{b} L_{ij}\left(f_i(\boldsymbol{r},t) - f_i^{eq}(\boldsymbol{r},t)\right) + F_i(\boldsymbol{r},t). \tag{6}$$

L_{ij} in Eq. (6) is a collision operator due to instantaneous collisions between particles. After collision process the populations are relaxed towards local equilibrium distribution, f_i^{eq}, which can be expressed in terms of the hydrodynamic variables $\boldsymbol{u}$ and ρ (the mass density) as follows:

$$f_i^{eq}(\rho,\boldsymbol{u}) = \rho a^{c_i}\left[1 + \frac{\boldsymbol{c_i}\cdot\boldsymbol{u}}{c_s^2} + \frac{(\boldsymbol{c_i}\cdot\boldsymbol{u})^2}{2c_s^4} - \frac{u^2}{c_s^2}\right] \tag{7}$$

where a^{c_i} are set of known weights which depend on the lattice model, and c_s is the speed of sound in the solvent. The last term, $F_i(\boldsymbol{r},t)$, in the Eq. (6) is a result of the momentum transfer from the polymer to fluid.

2.2.1 Coupling of Polymer and Fluid

As the fluid exerts a drag force on each bead of the polymer (according to Eq. (2)), an equal and opposite force should be applied to the fluid to conserve the total momentum. Since the fluid is modeled on the discrete grid while the polymer moves continuously, the fluid velocity $\boldsymbol{u_i}$ at bead position should be interpolated from the surrounding grid points. We employed simple nearest grid-point interpolation technique (trilinear interpolation) to obtain fluid velocity at the polymer position, in Eq. (2). In addition to the drag force, the random force in Eq. (3) should also be given to the fluid to satisfy the fluctuation dissipation theorem (FDT). Since the friction and random forces are available at the bead positions, we have to extrapolate them from the bead positions to the surrounding grid points. We used the same interpolation function that is used in interpolation of velocity, for this purpose. The total force density which is given to the fluid is written as:

$$\boldsymbol{f^{fl}}(\boldsymbol{r}) = -\sum_{i,r\in ng}(\boldsymbol{F_{drag,i}} + \boldsymbol{F_{ran,i}})\delta_r/\triangle x^3 \tag{8}$$

Here δ_r is the interpolation function, $\triangle x$ is the lattice grid spacing, and ng is the mess cell to which ith bead belongs. The source term, $F_i(\boldsymbol{r},t)$, in the Eq. (6) can be obtained from [9],

$$F_i(\boldsymbol{r},t) = \left(1 - \frac{1}{2\tau}\right)\rho a^{c_i}\left[\frac{\boldsymbol{c_i}-\boldsymbol{u}}{c_s^2} + \frac{(\boldsymbol{c_i}\cdot\boldsymbol{u})^2}{c_s^4}\boldsymbol{c_i}\right]\cdot\boldsymbol{f^{fl}}\triangle t \tag{9}$$

for each fluid population 'i'. Here τ is the relaxation time. The fluid density, and momentum are obtained from:

$$\rho = \sum_i f_i, \qquad \rho\boldsymbol{u} = \sum_i f_i\cdot c_i + \frac{\triangle t}{2}\boldsymbol{f^{fl}}. \tag{10}$$

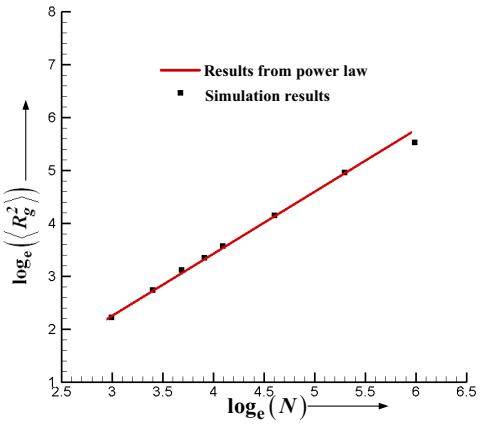

Fig. 2 Comparison of radius of gyration of a polymer.

The fluid density, and momentum are locally conserved in any collision process and the local equilibrium distribution functions should also satisfy the Eq. (10).

2.2.2 Thermal Fluctuations

Since we are dealing with microscopic scale problems, we have to consider thermal fluctuations in the fluid. In lattice Boltzmann method thermal fluctuations are included by adding stochastic collision operator, $\triangle'$, to the left hand side part of Eq.6. The fluctuating lattice Boltzmann equation can be written as [10]:

$$f_i(\boldsymbol{r}+\boldsymbol{c_i}\triangle t, t+\triangle t) = f_i^*(\boldsymbol{r},t) = f_i(\boldsymbol{r},t)+\sum_{j=1}^{b} L_{ij}\left(f_i(\boldsymbol{r},t)-f_i^{eq}(\boldsymbol{r},t)\right)+F_i(\boldsymbol{r},t)+\triangle'_i \tag{11}$$

Here $\triangle'_i$ is the random noise term that conserves mass and momentum. We can represent the collision matrix L_{ij} in diagonal form if we perform collision operation in moment space. Orthogonal basis vectors $\boldsymbol{e_{ki}}$, which are constructed from tonsorial polynomials of lattice vectors $\boldsymbol{c_i}$, are used to transform the distributions f_i into moments (modes) m_k. The non-equilibrium distributions $f_i^{n,eq}=f_i-f_i^{eq}$, in the collision term can then be expanded in moments as,

$$m_k^{n,eq}=\sum_i e_{ki} f_i^{n,eq}. \tag{12}$$

The collision operation can then be performed in moment space using linearized collision operator,

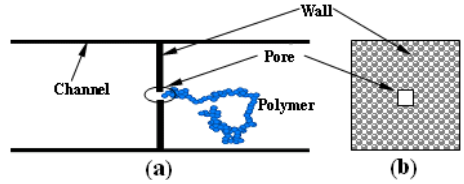

Fig. 3 Cross-sectional view of the simulation set-up at the center of (a) YZ-plane, and (b) XZ-plane.

$$m_k^{*n,eq}=\gamma_k m_k^{n,eq} \tag{13}$$

where $\gamma_k=1-1/\tau_k$ is the eigenvalue, which is depend on the relaxation time τ_k of each mode. The Thermel fluctuations are take into account by adding random noise to Eq. (13),

$$m_k^{*n,eq}=\gamma_k m_k^{n,eq} + \sqrt{\rho m_p w_k(1-\gamma_k^2)}\, r_k \tag{14}$$

here r_k being the Gaussian random number with zero mean and unit variance. The amount of thermal fluctuations can be controlled by mass of LB particle, $m_p=k_BT/cs^2$. After performing the collision operation the back transformation from moments to distributions is done by,

$$f_i^{n,eq}\equiv\sum_k a^{c_i} e_{ki} m_k^{n,eq}/w_k \tag{15}$$

where $w_k=\sum_i a^{c_i} e_{ki}^2$ is a normalizing factor of each mode.

3. Results and Discussions

3.1 Validation Tests

Before proceeding to simulation of the translocation process of the polymer, our numerical model is verified by comparing the radius of gyration of the polymer with the power law. The mean square radius of gyration is given by,

$$\langle R_g^2\rangle=\frac{1}{2N^2}\sum_{ij}\langle r_{ij}^2\rangle \tag{16}$$

with $r_{ij}=|\boldsymbol{r_i}-\boldsymbol{r_j}|$ being the inter-particle distance two beads.

The angular brackets indicate an ensemble average. The

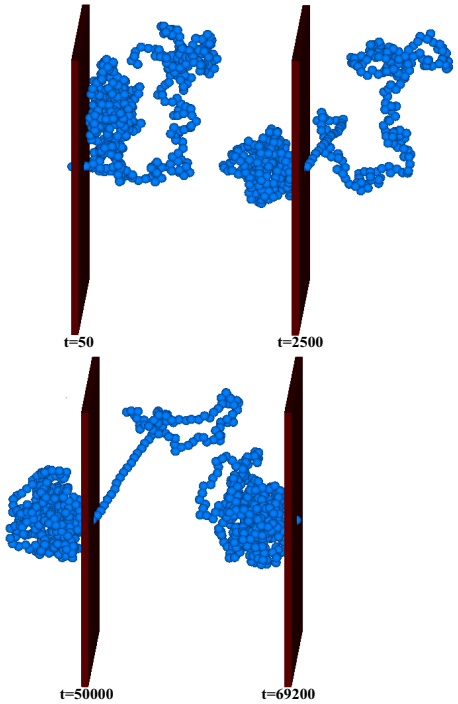

Fig. 4 Polymer configuration (N=400) of a translocation event at different times. The arrow indicates the driving force direction.

$\langle R_g^2 \rangle$ can be related to number of beads N by power law,

$$\langle R_g^2 \rangle \propto N^{2\nu} \tag{17}$$

where ν is called the Flory exponent. For self-avoiding walk (SAW) chains the Flory exponent is 0.588. We have computed the radius of gyration $\langle R_g^2 \rangle$ for different bead numbers using Eq. (16). To obtain statistically precise data, we calculated an ensemble average over 180 samples. Fig. 2 shows the log-log plot of $\langle R_g^2 \rangle$ vs N. The solid line indicates the results obtained from the power law(Eq. (17)), while the symbols indicate the results obtained from the simulation.

3.2 Polymer Translocation through a Nano-Pore

Fig. 3 shows the cross-sectional view of simulation set-up used in this work. The computations are performed in a square channel, which is opened in y-direction. A wall is located at the centre of the channel in x, z directions. At the centre of the wall a small pore is opened, which is of square cross-section.

In simulations all the parameters are given in lattice

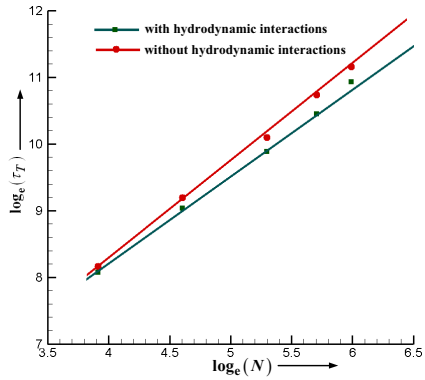

Fig. 5 Logarithmic plot of variation of translocation time with polymer length. The values of α are obtained from linear fit of data points.

units. For the polymer of length less than 200 beads, the dimensions of simulation box are set to be $40 \times 80 \times 40$ in x, y, and z directions respectively and for the length over 200 beads the dimensions are $50 \times 100 \times 50$. Initial position of the polymer is taken randomly from the self avoiding random walk algorithm (SARW), keeping the first bead position is at the entrance of the pore. Then the positions of the remaining beads are allowed to relax until it reaches to the equilibrium condition (temperature of polymer attains constant value), without hydrodynamic interactions (HI). Initial values for fluid velocity and density are taken to be zero and 1 respectively. This is then taken as a initial condition for the polymer translocation and simulations are carried out with and without HI. The boundary conditions for the polymer are periodic in y-direction, and the interactions with the solid walls are given by Lennard jones potential. For the fluid, periodic boundary condition is given in y-direction, and standard mid-plane bounce-back scheme is employed at the walls.

The size of the pore is taken as 3 and depth is set to be 1. At the beginning of the translocation process the polymer entirely resides in the left side of simulation box as shown in fig. 3. The translocation is then induced by applying a constant driving force in y-direction, which acting only on the beads that are in the pore region. The magnitude of the driving force is chosen such that it causes the fast (forced) translocation conditions. In fast translocation regime, the translocation time is far less than the Zimm time (relaxation time) of the polymer. Figure 4 shows the configuration of a polymer with 400 beads at different times of a translocation event. The arrow indicates the driving force direction. The simulation

parameters are taken from [11]. The lattice spacing $\triangle x$, and LB time step, $\triangle t$ are set to be unity. The ratio between LB time step and polymer time step is taken as 50. The driving force is taken as 0.01. The equilibrium distance between adjacent beads r_{eq} is 1.2. The strength of random force is controlled by temperature of the fluid, k_BT, which is equal to 10^{-04} in our simulation. The Lennard-Jones potentail parameters, σ, and ϵ are taken as 1.5 and 10^{-04} respectively. The force constant of bond stretching potential, K_{bond} is $2736\epsilon/\sigma^2$.

To know the nonlinear relationship between the translocation time, τ_T vs polymer length, which obeys a power law $\tau_T \propto N^{\alpha}$, the simulations are carried out for different chain lengths 50, 100, 200, 300, and 400. To reduce the statical uncertainty we have taken an ensemble average over 10 translocation events for each polymer length, with different initial configuration for each event. Fig. 5 shows the log-log plot of variation of translocation time with length of chain. The power law exponents, α obtained from our simulations are 1.29 ± 0.03, and 1.41 ± 0.03, with and without hydrodynamic interactions respectively. Our simulation results are in good agreement with the experimentally observed value of α, 1.27 ± 0.03 [12], especially when the hydrodynamic interaction effects are taken into account.

4. CONCLUSIONS

In this work, we have simulated the translocation process of a biopolymer thorough a nanopore in three dimensions. The polymer is modeled and simulated by Langevin dynamic techniques. The hydrodynamic interactions are taken into account by considering the solvent effect using lattice Boltzmann method. From the results, we obtained a nonlinear relationship between the translocation time and polymer length as $\tau_T \propto N^{1.29 \pm 0.03}$, which is in good agrement with the experimental results. If we neglect the hydrodynamic interactions the power law relationship is $\tau_T \propto N^{1.41 \pm 0.03}$. So we conclude that the hydrodynamic interactions play a crucial role in translocation process.

ACKNOWLEDGEMENT

This work was supported by the National Research Foundation of Korea through the NRL Program funded by the Ministry of Education, Science and Technology (Grant No.2005-1091).

REFERENCES

[1] 1981, Lamm, G. and Shulten, K., "Extended Brownian Dynamics Approach to Diffusion Controlled Processes," *J. Chem. Phys*., Vol.75-1, p.365.

[2] 1992, Hoogerbrugge, P. J. and Koelman, J. M. V. A., "Simulating Microscopic Hydrodynamic Phenomena with Dissipative Particle Dynamics," *Europhys. Lett.*, Vol.19, p.155.

[3] 1999, Malevanets, A. and Kapral, R., "Mesoscopic model for solvent dynamics," *J. Chem. Phys.*, Vol.110-17, p.8605.

[4] 1999, Ahlrichs, P. and Dunweg, B., "Simulation of a single polymer chain in solution by combining lattice Boltzmann and molecular dynamics," *J. Chem. Phys.*, Vol.111-17, p.8225.

[5] 2005, Usta, O. B., Ladd, A. J. C. and Butler, J. E., "Lattice-Boltzmann simulations of the dynamics of polymer solutions in periodic and confined geometries," *J. Chem. Phys.*, Vol.122, p.094902.

[6] 1971, Weeks, J. D., Chandler, D. and Andersen, H. C., "Role of repulsive forces in determining the equilibrium structure of simple liquids," *J. Appl. Phys.*, Vol.54, p.5237.

[7] 1992, Benzi, R., Succi, S. and Vergassola, M., "The lattice Boltzmann-equation－Theory and applications," *Phys. Rep.*, Vol.222, p.145.

[8] 2007, Premnath, K. N. and Abraham, J, "Three - dimensional multi-relaxation time (MRT) lattice-Boltzmann models for multiphase flow," *J. Comp. Phys.*, Vol.224, p.539.

[9] 2002, Guo, Z., Zheng, C. and Shi, B., "Discrete lattice effects on the forcing term in the lattice Boltzmann method," *Phys. Rev. E*, Vol.65, p.046308.

[10] 2009, Dunweg, B. and Ladd, A. J. C., "Lattice Boltzmann Simulations of Soft Matter Systems, in Advanced Computer Simulation Approaches for Soft Matter Sciences III," *Springer*, Vol.221, Germany p.89-166.

[11] 2006, Fyta, M., Melchionna, S., Kaxiras, E. and Succi, S., "Multiscale Coupling of Molecular Dynamics and Hydrodynamics: Application to DNA Translocation Throuugh a Nanopore," *Multiscale Model. Simul.*, Vol.5, p.1156.

[12] 2005, Storm, A., J., Storm, C., Chen, J., Zandbergen, H., Joanny, J. F. and Dekker, C., "Fast DNA Translocation through a Solid-State Nanopore," *Nano Lett. E*, Vol.5, p.1193.